



OPEN

The antiandrogenic vinclozolin induces differentiation delay of germ cells and changes in energy metabolism in 3D cultures of fetal ovaries

Silvia González-Sanz¹, Odei Barreñada¹, Eduardo Rial², Miguel A. Brieño-Enriquez^{3,4} & Jesús del Mazo^{1,4}✉

Vinclozolin is a pesticide with antiandrogenic activity as an endocrine disruptor compound. Its effects upon the progression of primordial follicles were assessed in cultures of mouse fetal ovaries from the onset of meiotic differentiation of germ cells (13.5 days post coitum) and from both in vivo exposed mice and in vitro exposed ovaries. Exposure of ovaries to vinclozolin—at in vitro dosages ranging from 10 to 200 μM and in 3D ex vivo culture following in vivo exposure to 50 mg/kg bw/day—showed delays in meocyte differentiation and in follicle growth, even at the lowest in vitro dose exposure. Immunofluorescent analysis showed the presence of the proteins MSY2 and NOBOX in the primary follicles but no difference in the level of protein signals or in the number of follicles in relation to treatment. However, assessing the cytological differentiation of germ cells by detecting the synaptonemal complex protein SYCP3, the exposure to vinclozolin delayed meiotic differentiation from both in vitro- and in vivo-exposed ovaries. These effects were concomitant with changes in the energy metabolism, detected as a relative increase of glycolytic metabolism in live-cell metabolic assays in exposed ovaries.

Mammalian oogenesis is a very complex process that requires perfect orchestration of intrinsic and extrinsic factors by germ cells in correlation with the surrounding granulosa and theca cells in the follicle^{1,2}. The correct differentiation of primordial germ cells (PGCs) in meiosis and the progression to primordial follicles by interactions between germ and somatic cells are crucial to determine oocyte fate, oocyte quality, the ovarian reserve, and in consequence reproductive lifespan^{3,4}.

In mouse ovaries, between 10.5 and 11.5 days post coitum (dpc), PGCs colonize the genital ridges. They then divide mitotically to increase the number of progenitor germ cells, initiating gonadal sex differentiation at about 12.5 dpc⁵. Mitotic division will continue within the ovary, where these divisions are characterized by incomplete cytokinesis, producing interconnected oogonia forming clusters of germ cells. Later, around 13.5 dpc, oogonia cells initiate meiosis and progress through meiotic prophase I up to dictyotene, remaining in that stage until meiotic resumption (after birth about 20 dpc). Meiotic prophase I is not fully synchronized, and during the first days of meiotic initiation, it is possible to observe mitotically active oogonia and oocytes having already entered meiotic prophase I during the first days of meiotic initiation⁶. The transition from cysts to individual follicles is initiated from 17.5 dpc, along with the beginning of follicular atresia, when only the surviving oocytes, as in other mammals, are surrounded by pre-granulosa cells^{7–9}.

Various chemical compounds present in nature or of anthropogenic origin can alter gametogenesis. A well-known group of such chemicals are the endocrine-disrupting chemicals (EDCs), which have previously demonstrated health risk, specifically as reproductive toxicants, as reported in 2013 by the United Nations Environment

¹Department of Cellular and Molecular Biology, Centro de Investigaciones Biológicas Margarita Salas (CIB-CSIC), Ramiro de Maeztu, 9, 28040 Madrid, Spain. ²Department of Structural and Chemical Biology, Centro de Investigaciones Biológicas Margarita Salas (CIB-CSIC), Ramiro de Maeztu, 9, 28040 Madrid, Spain. ³Magee-Womens Research Institute, Department of Obstetrics, Gynecology and Reproductive Sciences, University of Pittsburgh School of Medicine, Pittsburgh, PA, USA. ⁴These authors contributed equally: Miguel A. Brieño-Enriquez and Jesús del Mazo. ✉email: jdelmazo@cib.csic.es

Programme and the World Health Organization (*State of the Science of Endocrine Disrupting Chemicals – 2012*, www.who.int/ceh/publications/endocrine/en/index.html). The developmental dynamics of germ cell differentiation in mammalian females has hindered the analysis of some effects of the EDCs, particularly during the embryonic stages. Some critical studies have been carried out for specific EDCs in *C. elegans*^{10,11}, mice¹² and monkeys¹³. However, in mammals, the adverse effects of EDCs have been mainly assessed in males^{14,15}. While the incidence of reproductive disorders in females caused by exposure to EDCs, especially during fetal life, is much higher than initially estimated, it has scarcely been assessed in either mice or humans^{16,17}.

Ovarian function and folliculogenesis require a tight regulation and equilibrium of estrogenic and androgenic signals¹⁸. The effects of estrogens are well known but androgens have been more recently pointed out as crucial in ovarian function and folliculogenesis as well as one of the main causes of premature ovarian failure and polycystic ovarian syndrome¹⁹. Androgen production by granulosa and theca cells and their conversion to estrone and estradiol, mediated by BMP4-Smad signaling, have been recently identified in late folliculogenesis²⁰. However, the effects of abnormal levels of androgens during early oogenesis are poorly understood. Vinclozolin (VZN) [3-(3,5-dichlorophenyl)-5-methyl-5-vinyl-1,3-oxazolidine-2,4-dione] is a fungicide widely used in agriculture and considered an EDC pesticide with antiandrogenic effects, both by itself and its metabolites²¹, blocking the androgen binding site of the receptors²². The adverse effects of VZN have been studied in spermatogenesis from a range of perspectives, including altered transgenerational effects on PGCs^{23,24}. However, very limited studies have been performed on the effect of antiandrogen EDCs, particularly on VZN²⁵, in oogenesis and early folliculogenesis.

Using *in vivo* and *in vitro* 3D cell culture systems²⁶, we analyzed the disruptive effects of VZN on the development of the mouse ovary. We used ovaries from animals unexposed or exposed to vehicle (DMSO) (controls) and animals exposed to various concentrations of VZN. In particular, we evaluated the regulatory effects of VZN on the meiotic differentiation of PGCs, on folliculogenesis, and for the first time, on the mitochondrial energy metabolism of the female germ cell line, from PGCs to primary follicle. The results revealed both unexplored characteristics of normal development, such as in meiosis, and changes induced by the environmental pollutant VZN. Our study utilizing 3D cultures of fetal ovaries as a model, reveals that VZN affected the meiotic progression of PGCs and early folliculogenesis, leading to a delay in differentiation concomitant with an increase in the glycolytic pathway.

Results

Cytological and morphometric analysis of follicular progression *in vitro*. Morohaku et al.²⁷ established a protocol to obtain *in vitro* mouse oocytes from PGCs. However, the approach precludes a cytological²⁸ and metabolic assessment of the differentiation process and analysis of the effects of potentially toxic compounds as we have performed. For these reasons, we have modified some aspects of the protocol, mainly the supports of the 3D cultures. The modifications made to the initial culture protocol did not affect the established progression of cell differentiation and folliculogenesis in mouse ovaries in the developmental window from 13.5 dpc followed by 17 days of culture (Fig. 1). The modifications of the culture procedures allowed us to perform functional analyses of the processes from 3D *in vitro* cultures and evaluation of the effects of potential reproductive toxicants, such as the endocrine disruptor vinclozolin (VZN), delivered *in vitro* during the culture process or by the culture of ovaries previously exposed *in vivo*. This approach facilitated a continuous analysis of differentiation during any window during the 17 days of culture in physiological conditions with cell–cell interactions, enabling the cytological and metabolic assessment, which are difficult to establish by other traditional methods.

To understand the follicular developmental pattern, the mouse *in vitro* cultures were initiated at 13.5 dpc instead of 12.5 dpc²⁷ to ensure that the meiotic process had begun²⁹. For the monitoring of cultures, measurements of two perpendicular diameters of each follicle in every type of exposure and control were taken every 2 days, from Day 9 to Day 17 of culture. The morphological progression of follicles from the control groups matched the progress of those analyzed *in vivo*³⁰ (Fig. 1). Ovarian cultures from both VZN-exposed embryos *in vivo* (through maternal exposure) and ovaries exposed *in vitro* during the culture progression were assessed by measuring the diameter of follicles in whole mounted ovaries compared with the respective controls.

***In vitro* exposure.** First, we evaluated whether the presence of the VZN vehicle (DMSO) in the culture media alters the development of follicles. We compared the follicle size in the two types of controls: with (DMSO) and without the vehicle in the medium (control standard or ST). Our results showed that, on Day 9, the follicles growing at control ST conditions presented an average diameter of 43 μm , whereas, in the ovaries exposed to the vehicle, the average was 40.1 μm , without significant statistical difference. There continued to be no statistically significant differences between both types of controls throughout the culture progression (Fig. 2).

In order to establish a potential dose–effect correlation of VZN exposure, the analysis of follicular development was carried out with *in vitro* exposure to 10 μM , 50 μM , 100 μM , and 200 μM concentrations of VZN in the culture medium. Overall, we observed that follicular size evidenced a progressive and continued growth both in controls and in the follicles exposed to the various concentrations of VZN. However, follicle size was decreased at all VZN treatment levels (Fig. 2A); and, there was no correlation between dose level and follicle size during the *in vitro* experiment ($R^2 = 0.117$). Results indicate that VZN delayed follicle progression and reduced follicle size during *in vitro* exposure. The lack of a dose–response during exposure suggests that the lowest dose, 10 μM , elicited the maximum attainable response.

***In vivo* exposure.** We evaluated the follicle diameters in ovarian explants taken from control and VZN-treated mice after 9 to 17 days in culture. No significant differences were found in the size of the follicles between the two control groups (DMSO and Control ST) (Fig. 2B). However, at day 9, follicle diameters already revealed

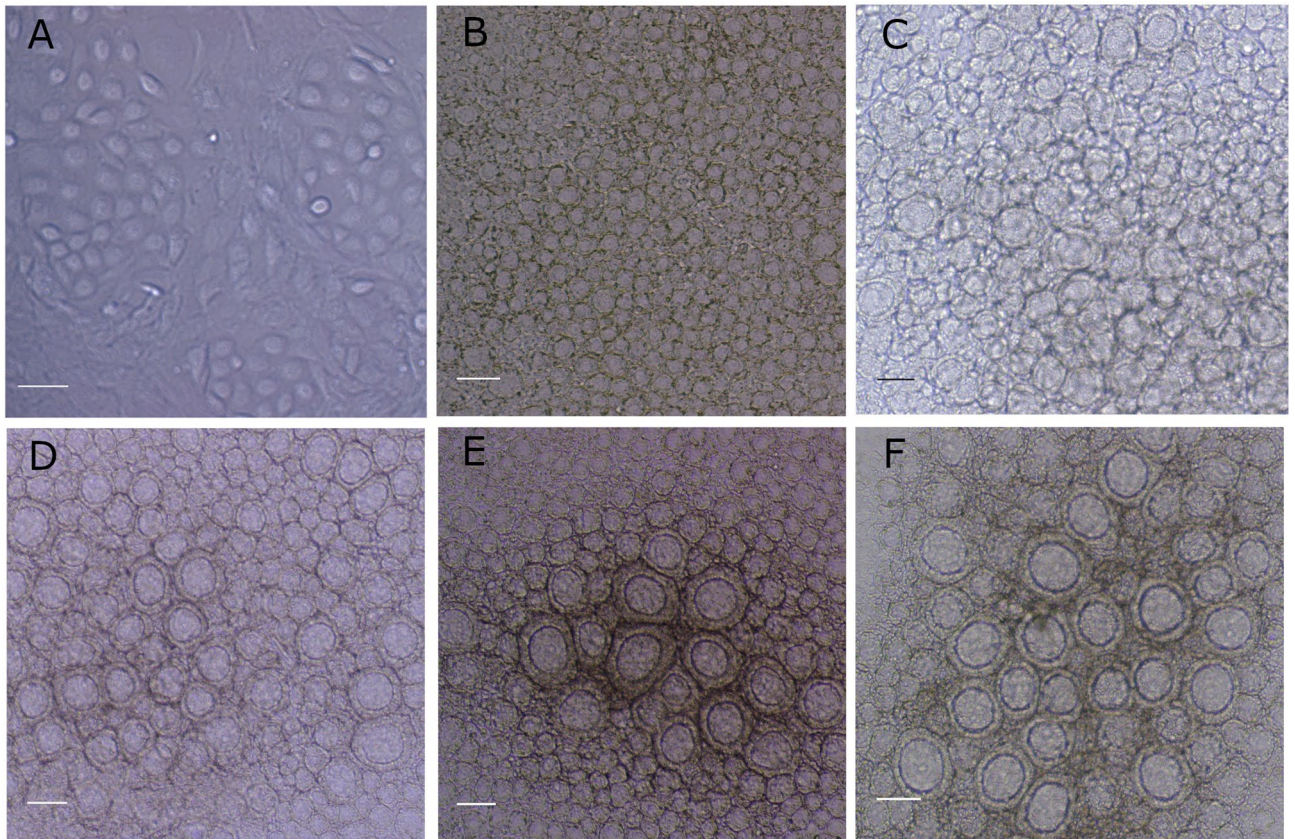


Figure 1. In situ microscopy contrast phase images of the progress of follicles in control conditions from ovary cultures initiated at 13.5 dpc: after 2 (A), 9 (B), 11 (C), 13 (D), 15 (E), and 17 (F) days of culture. Bars represent 50 μm .

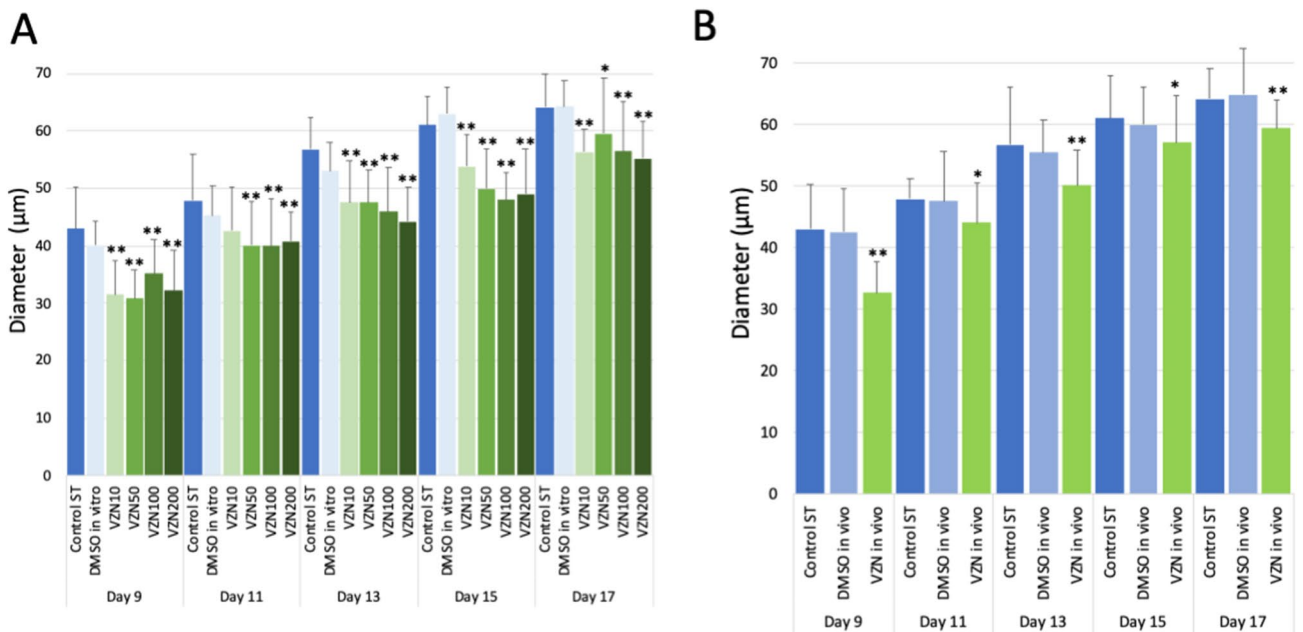


Figure 2. Follicle size at various days of VZN exposure. (A) In vitro exposure at various concentrations of VZN. Bars represent the mean of 2 to 6 replicates with each replicate containing 15–109 follicles in each experimental condition. (B). In vivo exposure to VZN. Bars represent the mean of 2 to 6 replicates with each replicate containing 39–152 follicles in each experimental condition. Statistical significant differences are indicated by * ($p \leq 0.05$) or ** ($p \leq 0.01$), in comparison to the respective DMSO controls.

differences between the follicles exposed *in vivo* to VZN compared to controls. While the controls showed an average diameter of 42.6 μm , the follicles exposed to VZN *in vivo* showed 32.7 μm ($p \leq 0.01$, Fig. 2B). Size of follicles from VZN-treated mice remained significantly reduced for the duration of the culture period ($p \leq 0.05$). These results indicate that *in vivo* exposure to VZN results in smaller follicles in the mouse ovary.

Cytological analysis of germ cell progression and effect of VZN in 3D cultures. To validate the morphometric analysis of follicle progression and to evaluate potential changes in meiotic development as critical biomarkers during such progression, different functional proteins were analyzed by immunofluorescence assays.

We analyzed the presence of MSY2 (a germ-cell-specific member of the Y-box family of DNA-/RNA-binding proteins), initially only present in the cytoplasm of female germ cells, with a fundamental role in the regulation of mRNA stability³¹. It has been described as exclusively detectable in oogenesis after the dictyotene stage^{32–34}. However, observation of our 3D cultures indicated that the presence of the MSY2 protein was already apparent from early stages of primordial follicle differentiation. In addition, a weak MSY2 signal was detected in the cuboidal granulosa cell layer (Supplementary Figure 2). This could also support the active communication between oocytes and granulosa cells³⁵. Moreover, in the initial preantral stages, MSY2 localization is coherent with cystic functional organization of the oocytes and the physiologic situation of the syncytial structure in clusters, with wide cytoplasmic communication (Fig. 3, Day 5; Fig. 4A). Nevertheless, we detected no differences in the patterns of MSY2 signaling between ovaries exposed, *in vitro* or *in vivo*, to VZN and controls during culture progression, indicating that the expression of MSY2 was not altered by VZN.

Due to the differences found in the follicular size of gonads exposed to VZN in relation to controls, we decided to analyze a marker of meiotic prophase I progression of the oocytes in culture. Synaptonemal complex protein 3 (SYCP3) is an essential structural protein of the lateral elements of the synaptonemal complex (SC)³⁶. By double immunolabelling with anti-SYCP3 and anti-MSY2, it was possible to cytologically validate the association between the SYCP3 marker and germinal cells (Fig. 4A).

SYCP3 is able to clearly define the cytological progress of meiotic prophase I. Surprisingly, by using SYCP3 immunodetection *in toto* in 3D fetal ovarian culture, we identified how SYCP3 progressively accumulated in discrete nuclear structures as the lateral elements became disorganized during desynapsis. It was reported, by temporal localization, that elements recognized by anti-SYCP3 could be localized in meiosis at nucleolar regions³⁷. To verify whether the accumulated SYCP3 detected in our study was incorporated into the nucleoli, we used double immunolabeling to detect its colocalization with anti-nucleolin antibody (used as marker for the nucleolus). A high level of colocalization of both proteins was observed (Fig. 4B) (a colocalization value of 87%, quantified by Leica superposition and image comparison software). No differences in nuclear localization were detected between controls and VZN exposed ovaries. Hence, these results validated previous observations and suggested the participation of nucleoli in the pathway of disorganization of the lateral elements of SCs, at least in female meiosis.

To test whether there was a delay in the meiotic process after exposure to VZN, concomitant with the delay detected in the progression of follicle sizes in the exposed ovaries, the proportion of cells in different meiotic stages of prophase I were recorded on days 5, 7, and 9 of culture in both controls and VZN exposed ovaries. Meiotic stages were cytologically identifiable by the SC structures (Fig. 4C) in leptotene, zygotene, early pachytene, late pachytene, and late diplotene/diakinesis. The absence of structured SCs in the last stages of this differentiation was also recognized by the SYCP3 accumulation colocalized with nucleoli. VZN exposure delayed the progress of meiocytes; however, cytologically, they recovered at diakinesis after day 9 of culture. After *in vitro* exposure to VZN, meiotic differentiation was significantly delayed at all exposure levels (Fig. 4D,E). These analyses indicate that *in vitro* and *in vivo* exposure to VZN elicited a delay in meiotic differentiation.

Analysis of the energy metabolism. ATP is produced in the cell by two coordinated processes, oxidative phosphorylation and glycolysis. The study of the contribution of these two processes to the cellular energy metabolism during oocyte maturation³⁸ may be pivotal to understanding metabolic changes associated with proliferation, differentiation, or cellular dysfunction of female germ cells. The rates of respiration and lactate formation were measured during oocyte progression *in vitro*³⁹ in exposed and control cultures (Fig. 5A, B).

Mitochondrial respiration was initially stable following *in vivo* or during *in vitro* exposure to VZN (Fig. 5C,D). On day 12 of culture, mitochondrial respiration decreased in VZN-treated gonads (Fig. 5C) that, however, did not affect the maximal respiratory capacity (Fig. 5D). Interestingly, the decrease in the basal respiratory rate was compensated by an increase in the rate of glycolysis (Fig. 5E) thus suggesting that the decrease in mitochondrial ATP production is compensated by an increase in glycolytic ATP formation. Therefore, these results reveal a metabolic change on day 12 that appears as a Warburg-like effect, that is clearly evidenced by the low OCR/ECAR ratio (Fig. 5F). To evaluate whether these metabolic changes could affect folliculogenesis during the early stages, we assessed, by immunofluorescence, the relative follicle concentration using the anti-NOBOX antibody at day 12 of culture after *in vitro* VZN exposure. NOBOX protein (newborn ovary homeobox gene) is crucial in early folliculogenesis⁴⁰ and preferentially expressed in growing oocytes of the primordial follicles through metaphase II⁴¹. We used NOBOX as marker for growing oocytes to assess the follicle population after the different VZN exposures and controls. No apparent differences in relative follicle concentration were detected in the images (Fig. 5G). Finally, we evaluated metabolism on day 15 of culture. Interestingly and in agreement with the results by NOBOX immunofluorescence data, we observed that the OCR/ECAR ratio returns to control values, indicating that this metabolic change is transient in this period of development. Consequently, VZN exposure could metabolically affect to the oocytes in a crucial window during early differentiation associated to meiotic differentiation as we has also been detected.

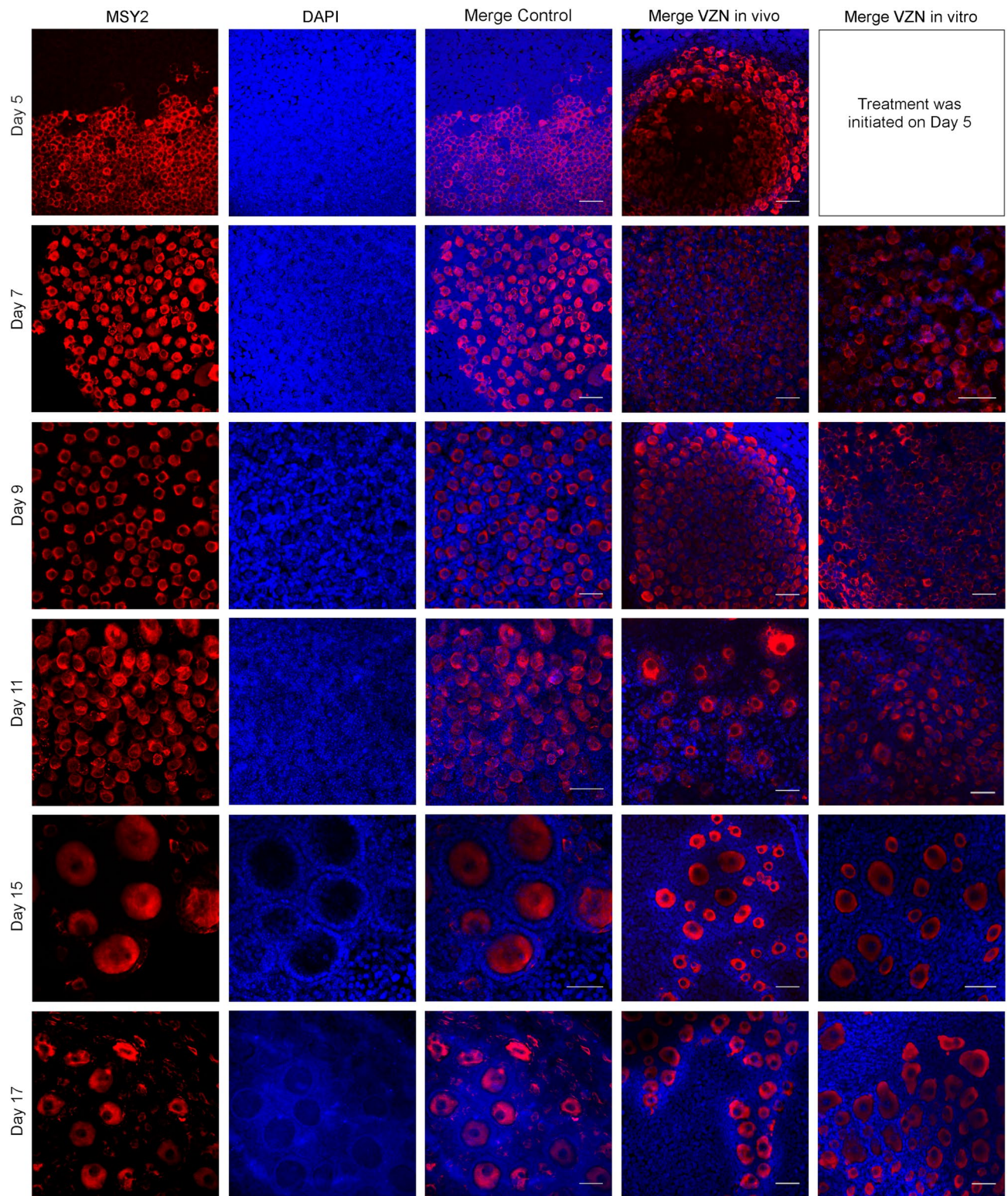


Figure 3. Changes in the localization of MSY2 during follicular progression during culture, DMSO controls (first three columns), in in vivo and in vitro ($10\ \mu\text{M}$) exposures to VZN (as VZN exposure is initiated at day 5 of culture the first image of in vitro exposed cultures corresponds to day 7 of culture). Bars represent $50\ \mu\text{m}$.

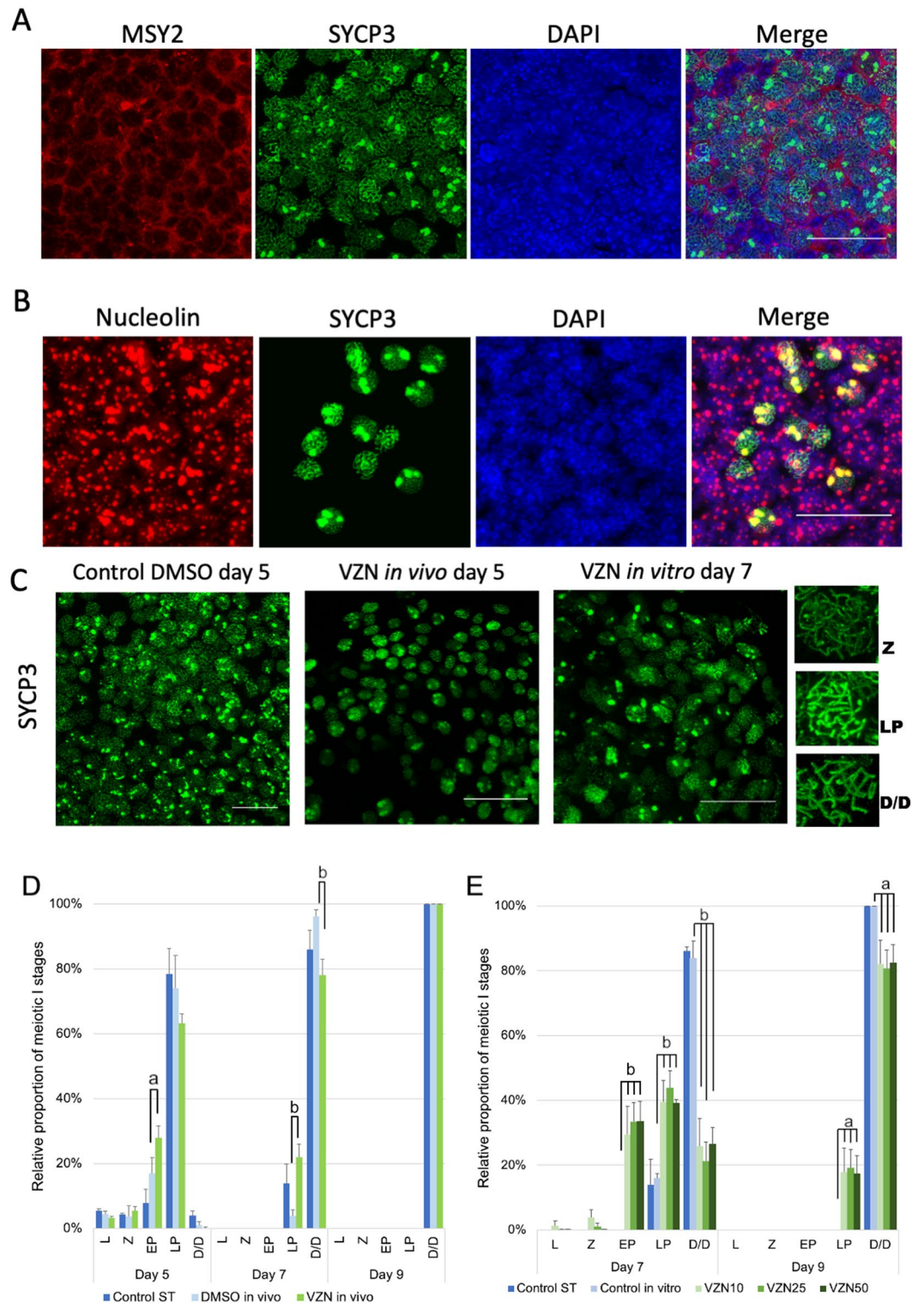


Figure 4. In toto immunostaining of cultured ovaries and analysis of meiotic progression. (A) Immunofluorescence localization of MSY2, SYCP3, and DAPI staining in meicytes at day 5 of DMSO control culture. (B) Colocalization of SYCP3 and nucleolin proteins in meiotic cells SYCP3 staining. Discrete nuclear structures of lateral elements of the synaptonemal complexes are detected colocalizing with nucleoli staining during desynapsis. (C) Representative images of SYCP3 immunostaining of controls and VZN exposed cultures; as VZN exposure is initiated at day 5 of culture the image corresponds to day 7 of culture. Z = zygotene, LP = late pachytene and D/D = diplotene/diakinesis. Bar represent 25 μm. (D, E) Proportional distribution of different stages of meiotic cells in prophase I during the progress of ovarian cultures. (D) In vivo exposure to VZN. (E) In vitro exposure to VZN. Day 5 is not represented in this figure as the exposure to VZN in vitro began on day 5 of culture. Bars represent the mean of two biological replicates (ovaries) + SD [(C) 100–611 follicles per replicate; (D) 100–427 follicles per replicate]. Statistically significant differences respect the metabolic basal condition are indicated as: “a” correspond to *p* value ≤ 0.05 and “b” to *p* value ≤ 0.01.

Discussion

Evaluation of endocrine disruptors and other toxicants in ovary development has been very much limited by the lack of methods for the study of in vitro processes that occur during fetal development in the whole ovary. In this study we used different methodological approaches that facilitate the evaluation of potential toxicants, which could affect early stages of female gametogenesis, by a combination of cytological and other analyses, including mitochondrial energetic metabolism.

These approaches also allow us to reveal biological processes in the context of the ovary in its entirety during development. In this context, we have determined how some components of the synaptonemal complex accumulate in the nucleoli during the meiotic progress. Some links between the synaptonemal complex and nucleoli have been previously reported⁴². Pachytene checkpoint protein 2 (Pch2) is a protein required for the checkpoint of meiotic cell-cycle progression in response to defects in recombination; it is localized into the nucleolus with suggested participation in the control of ribosomal DNA recombination. But it is not surprising that proteins that have fulfilled their function, as those that have shaped the synaptonemal complex structures, might be rapidly sequestered in the nucleolus as other critical proteins participate in very precise and time-dependent processes, to avoid interference with other targets in the cell cycle or differentiation, generating a signaling pathway between nucleolar proteins and cellular checkpoints⁴³. However this specific accumulation of SYCP3 at the diplotene stage in female meocytes should be studied in more detail in the future.

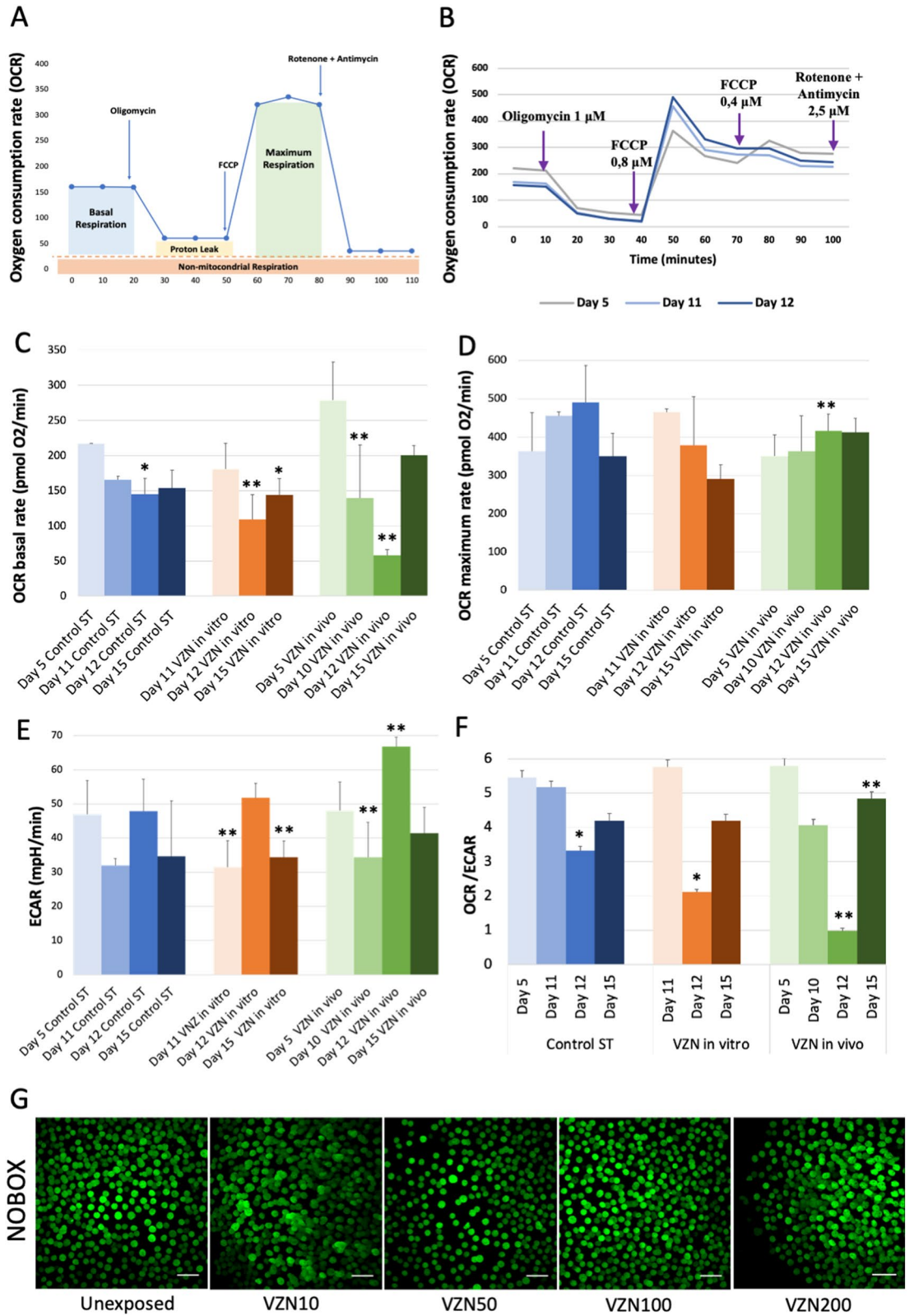
The effects of antiandrogenic compounds, such as vinclozolin, have been widely studied during the spermatogenic process, affecting not only the individuals directly exposed but also generating transgenerational alterations transmitted by epigenetic mechanisms, including changes in DNA methylation and microRNA expressions^{23,24,44,45}. However, studies on the effect of antiandrogens during development of mammalian female gonads are scarce^{25,46}, particularly during the crucial process of embryonic germ cell differentiation.

In vitro culture of mouse ovaries for 12 days, starting from 13.5 dpc, as in the present study, is an equivalent period in vivo to the perinatal time, which corresponds to a key period in oocyte development, including the attrition that is initiated during PGC and meiotic prophase by apoptosis^{47–49}, but reaches the height of its expression in the perinatal period⁵⁰.

Meiotic initiation in female germ cells is induced by high levels of retinoic acid, expressed outside the germ cells in some somatic tissues of the embryo such as in the mesonephros⁵¹, by stimulating the expression of *Stra8* (stimulated by retinoic acid 8)^{52,53}. The meiotic progression in the performed in vitro cultured ovaries, detected by MSY2 and SYCP3, suggests that the signals necessary for such progression were not affected by the absence of the mesonephros, which we removed before culture initiation. That is, all signals involved in such commitment seem to have been transferred to the ovary previous to the start of the in vitro culture of the ovaries. However, the decline in the progression size of preantral follicles detected as an effect of VZN exposure could be interpreted as a lack of nexus between potential mesonephros signals and ovary cells. Alternatively, such deficiencies could be attributed to the metabolic pathways of the proper ovary.

The delay in meiotic progression and follicle growth seems to be affected by the antiandrogenic effect of VZN. Androgen receptors (AR) are present in the fetal ovary⁵⁴. The meocytes could suffer a temporary arrest in pachytene/diplotene, which is related to the smaller size detected in the primordial follicles. The role of theca cells in synthesizing androgens and transporting this signal to granulosa cells⁵⁵, acting as the substrate for aromatase⁵⁶, could be interfered with by the presence of antiandrogens such as VZN. In mammalian males the action of androgens is critical in spermatogenesis. Deprivation of androgens alters the first meiotic division of spermatocytes^{57,58}. The meiotic checkpoint is subject to stricter controls in males than in females. The role of androgens in such a key checkpoint in oocyte meiosis is unknown⁵⁹. Our results could indicate that the depletion of androgens by blocking AR might mediate such a difference, based on the observed effects of the antiandrogenic VZN at very low concentration in vitro, able to interact with the limited number of receptors in the ovary. This is demonstrated in the various AR knockout (ARKO) mouse models, in which the phenotypes in males were more severe than in females⁶⁰.

The role of the mitochondrial activity in oocytes is very crucial considering their increase in number during oogenesis and their stability during early development⁶¹. Androgen precursors may contribute to the synthesis of estrogens, mediated by aromatase (CYP19)⁶². Estrogens are involved in mitochondrial metabolism and function⁶³. Mitochondria is a prevalent target of EDCs⁶⁴. Alteration of energy metabolism by mitochondrial dysfunctions has been associated to the exposure to several EDCs^{65,66}. About 800 EDCs are considered as disrupters of mitochondrial membrane potential⁶⁷. VZN has not been previously assessed as disrupter of mitochondrial function, neither in relation with cellular alteration of folliculogenesis in early ovarian development. To assess the differentiation of the oocytes and the progress of folliculogenesis in this 3D culture model, as well as the potential effects of this EDC on mitochondria, we evaluated the energy metabolism dynamics during the differentiation process, both in controls and in VZN exposed ovaries. The results obtained in whole ovaries after 12 days of culture (equivalent to the birth developmental window) indicate a transitional change, both in vitro and in vivo, in the metabolic pathway with a decrease in mitochondrial respiration and increasing lactate production. However, our results demonstrated that this change was not due to any decrease in the number of mitochondria. Such anaerobic glycolysis might compensate for the reduction of oxidative phosphorylation. This change corresponds, in vivo, to perinatal age with resumption of meiosis, which is initiated in the mouse. The cumulus cells surrounding oocytes have a clear role in oocyte growth and maturation, which metabolize glucose, producing glycolytic metabolites⁶⁸. Glucose is mainly metabolized via glycolysis in oocytes by the pentose phosphate pathway⁶⁹. This has the consequence of relative mitochondrial inactivity to avoid oxidative stress during the differentiation process of germ cells⁷⁰. Our results, in ovaries treated in vitro or in vivo with VZN, indicate that exposure, in early development, to this pesticide may alter the reprogramming of the metabolic pathway via glycolysis and, hence, the normal differentiation in this critical period of folliculogenesis, with consequences in the ovarian reserve in adults. A



◀ **Figure 5.** Energetic metabolism analysis. **(A)** Scheme of the parameters evaluated in the 3D cultures of fetal ovaries by the Mito Stress Test. **(B)** Mitochondrial oxygen consumption rate (OCR) on key representative days during the progress of the culture in control conditions. **(C, D)** Mitochondrial oxygen consumption rate (OCR) in ovaries exposed in vitro or in vivo to VZN. **(C)** Basal rate. **(D)** Maximum rate. **(E)** Quantitative measurement of basal glycolytic rate using extracellular acidification rate (ECAR) parameter, in controls cultures and in VZN-exposed ovaries. **(F)** Ratio between mitochondrial respiration and basal glycolysis in controls and in ovaries exposed in vitro or in vivo to VZN. Bars indicate the mean of 3–6 biological replicates (ovaries) \pm SD. Statistically significant differences respect the metabolic basal condition are indicated as: * correspond to p value ≤ 0.05 and ** to p value ≤ 0.01 (ANOVA, Tukey's and Dunnett's test); (basal conditions correspond to day 5 in in vivo exposures but basal condition for in vitro exposure is day 5 control ST since it is on day 5 when experimental in vitro exposure to VZN began). **(G)** NOBOX in toto immunostaining of oocytes on day 12 of culture in DMSO controls and in vitro exposed with the different VZN concentrations experimentally used. Bar represents 50 μ m.

similar situation of lactate increase by upregulation of the glycolytic pathway has been detected in the alteration of oocytes and follicle development in polycystic ovary syndrome patients⁷¹. However, the oocyte density at the time of glycolytic increase on Day 12 does not seem to be greatly affected according to our immunocytochemical experiment using the anti-NOBOX antibody and subsequent cytological analysis and could be an acute response mechanism to the toxic effect of VZN specifically at a critical point in cell differentiation.

As we show in this study, culture of the ovaries in 3D conditions from early developmental stages can facilitate a more accurate analysis of the process of oogenesis and folliculogenesis in the whole ovarian tissue environment during development.

The experimental approaches used in the analysis of the effects of toxic agents that alter germ cell differentiation and progress, might illuminate potential consequences of different toxicants in adult female fertility. The application of methodological updates introduced in the present study and the comparative results obtained in vivo and in vitro demonstrate this possibility.

Materials and methods

Animals. CD1 mice were the models used in this research. The experimental approaches were carried out according to the Royal-Decree Law RD53/2013 about the use and care of animals in experimentation. All assays performed had the approval of the Committee of Bioethics of Animal Experimentation of CIB-CSIC and also of the Autonomous Community of Madrid (PROEX 054/15).

Development of female gonad cultures. The global experimental approach is schematized in Supplementary Figure 1. Embryos were obtained from pregnant females at 13.5 dpc. After dissection, the uteri of pregnant females were washed in L-15 Leibovitz media (Sigma-Aldrich) supplemented with 5% fetal bovine serum (FBS, Sigma-Aldrich) and 10 units/ml penicillin–streptomycin (Gibco). Using a stereomicroscope, we dissected the embryos and collected the gonads attached to the mesonephros, which were removed from the gonad using tungsten needles just before the seeding of the gonad. Our culture method for the ovary was based on the protocol described previously by Morahaku et al.^{26,72}. However, in order to perform in-depth cytological, in situ immunofluorescence, and mitochondrial activity studies, we modified the method of the culture procedure depending on the process to be evaluated—follicular progression, immunofluorescence, or mitochondrial activity. The basic amendments to the original protocol were the replacement of the support of the culture from plates with Transwell-COL membranes to: 24-well polystyrene culture plates (Falcon) to evaluate the progression on follicles; 12-chamber glass slides (Ibidi) for the immunofluorescence analysis; and specific cell culture miniplates (Agilent Seahorse XFp) for assessment of mitochondrial activity of the ovaries in toto.

To evaluate the follicular progression of the culture by cytological analysis in toto, before the distribution of the gonads in the P24 plates, 125 μ L of alpha-MEM (minimum essential medium) stock A (alpha-MEM, 2-O-alpha-D-glucopyranosyl-L-ascorbic acid and 0.1% vol/vol penicillin–streptomycin) was added to each well. Each gonad was divided into halves and settled in the wells for 1 h at 37 °C under 5% CO₂, 95% air. Subsequently, wells were refilled with the same medium up to 250 μ L each. After 5 days of culture (equivalent to 18.5dpc in vivo), the medium was replaced with new medium containing the estrogen receptor antagonist ICI 182,780 (R&D Systems)²⁷ at a final concentration of 5 μ M until Day 11 of culture (equivalent to perinatal period in vivo), which was replaced by alpha-MEM stock A until Day 17 of culture (equivalent to about 10 days postnatal). During all culture periods, the media was changed every 2 days, replacing half of the volume (125 μ L) with fresh medium.

Immunofluorescence. For immunofluorescence analysis, chamber slides with removable 12-well silicone chambers (Ibidi) were used. The day before the isolation of the gonads from the embryos, each well was covered with collagen due to the limited capacity of the explants to adhere to the glass. Collagen type I from rat tail (Merck) was diluted in 0.1 M NaHCO₃ at a 34 μ g/ml concentration, sterilized by filtration, and 200 μ L of the solution was added to each well. Plates were incubated overnight at 37 °C, 5% CO₂, 95% air, followed by replacement of collagen by supplemental alpha-MEM culture medium, washing each well two times with the same medium. The gonads, divided into halves, were settled in each well with 50 μ L of alpha-MEM stock A. The explants were incubated overnight at 37 °C, 5% CO₂, 95% air, until they adhered to the surface of the well. The medium changes were performed every 2 days, maintaining the same time period as for the ICI treatment.

Energy metabolism. To evaluate energy metabolism, the Extracellular Flux Analyzer XFp (Agilent Seahorse) was used during the progression of the developing ovary explants. Individual ovaries (divided into three equivalent fragments) were cultivated in Seahorse XFp miniplates supplemented with alpha-MEM Stock A. The plates, containing three equidistant fragments in each well, were initially incubated in 15 μ L of medium at 37 °C, 5% CO₂, 95% air for 1 h to allow adherence of the tissue to the surface of the wells. Each well was filled with 40 μ L of medium. Two of the eight wells of the plate were used as background controls for the assay. The protocol of culture was performed as indicated above.

Assessment of the bioenergetic profiles of the ovary explants was performed using the Mito Stress Test Kit (Agilent Technologies for Seahorse XFp), in which known compounds acting on the oxidative phosphorylation system were used. The mitochondrial respiration and glycolytic activity were determined from the oxygen consumption rate (OCR) and extracellular acidification rate (ECAR, a proxy for the rate of lactate production), respectively.

On the day of the analysis, the culture medium was changed to 180 μ L of bicarbonate-free DMEM (Sigma-Aldrich) supplemented with glucose 5 mM, 2 mM L-glutamine, 1 mM pyruvate, 2% FBS (Sigma-Aldrich), and HEPES 5 mM pH 7.4. Cells were maintained for 1 h in a CO₂-free incubator.

The experimental setup was based on a predesigned program called “Mito Stress Test” (Agilent) with slight modifications. After taking four measurements under basal conditions, three measurements were made in the presence of oligomycin 1 μ M to inhibit mitochondrial ATP synthesis. Subsequently, measurements were made in the presence of two concentrations of the uncoupler FCCP (carbonylcyanide-p-trifluoromethoxyphenylhydrazide, 0.8 μ M and 1.2 μ M final) to determine the maximum respiratory rate. Finally, three measurements were made in the presence of rotenone and antimycin (2.5 μ M of each inhibitor) to inhibit mitochondrial respiration.

Exposure to vinclozolin (VZN). To perform reprotoxicological assays, two types of exposure were carried out: a) *in vitro* exposures and b) *in vivo* exposure followed by *ex vivo* culture (Supplementary Figure 1). Considering that VZN can be metabolized in the liver and that *in vitro* biotransformation by liver microsomes has been tested at 50 μ M concentration⁷³, we have analyzed a wide range of VZN concentrations in ovary cultures. For *in vitro* exposure, cultures were treated with various concentrations of VZN (10, 25, 50, 100, and 200 μ M in 0.1% DMSO) in the medium from day 5 (equivalent *in vivo* to 18.5) to day 11 of culture (equivalent *in vivo* to 19.5–20.5 dpc, that is about birth time), together with the ICI treatment. Controls were exposed to 0.1% DMSO; an additional *in vitro* control of 1% DMSO was also evaluated. *In vitro* doses of VZN were based on previous analyses testing steroidogenesis in exposed culture cells at non-toxic concentrations ranged from 0.3 to 300 μ M VZN in the same vehicle (0.1% DMSO)^{22,74}.

In rodents, the developmental lowest observed adverse effect level (LOAEL) was established at 50 mg/kg/day⁷⁵. In the present study, to evaluate *in vivo* exposure, pregnant female mice were exposed, by drinking water, to the LOAEL dose of 50 mg/kg bw per day of VZN (Sigma) dissolved in DMSO (Sigma) (1.1 g/kg/day) from plug detection (0.5 dpc) until euthanasia at 13.5 dpc. The same dosage of DMSO was used as a control (as well as controls without DMSO [control ST]). This VZN dosage has been previously used in female mice to investigate the effects during embryogenesis⁷⁶, although effects in rodents has been detected at 100–200 mg/kg bw/day of VZN^{77–79}, an increase in polycystic ovaries in F3 offspring generation after 100 mg/kg bw/day exposure in F0 was also detected⁸⁰. Cultures were performed as indicated above.

Cytological and morphometric analysis of *in vitro* follicular progression. Follicle growth is good biomarker of follicle development⁸¹. During follicular development, photographs were taken using *in situ* microscopy phase contrast along the culture progression, starting in all cases from 13.5 dpc ovaries, with a Nikon Eclipse TE300 microscope equipped with a Nikon DXM1200 camera and the ACT-1 for DXM1200 and DXM1200F programs. Follicle size was analyzed by measuring and averaging two perpendicular diameters of all follicles displayed in randomly selected microscopic areas of the cultures³¹, using the ROI Manager tool from the ImageJ program. A total of 2775 follicles were measured. An average of 69 follicles were analyzed per each selected day after culture initiation and exposure. Dispersion analysis was carried out to confirm that the number of follicles analyzed did not show correlation with data dispersion. That is, samples showed similar dispersion although the number of cells analyzed was different.

Immunofluorescence assay. The explants cultured directly on slides with removable 12-well silicone chambers as indicated above, were rinsed in phosphate-buffered saline (PBS) with 0.1% Triton-X 100 after removing the culture medium and the silicone wells. Fixation of the tissues was performed by sequential incubation in 1%–2%–4% paraformaldehyde in PBS with 0.1% Triton X-100 for 1 h at room temperature. Then, the tissue was rinsed three times with PBS/0.1% Triton-X 100, followed by blocking with 5% bovine serum albumin during 30 min, incubated overnight with primary antibodies at 4 °C in blocking solution in a humidified chamber, washed three times for 15 min, and incubated 1 h with secondary antibodies. Finally, the silicone chambers were removed, and the slides were washed 3 times for 15 min and mounted in DAPI UltraCruz mounting medium (Santa Cruz Biotechnology). The primary antibodies were: mouse anti-SYCP3 (Santa Cruz Biotech.) at 1:500 dilution in PBS; rabbit anti-MSY2 (gift from R. Shultz, Univ. Pennsylvania) at 1:1000; goat anti-NOBOX (gift from A. Rajkovic, Univ. of Pittsburgh) at dilution 1:100; and rabbit anti-nucleolin (Abcam, 1:100). Secondary antibodies were: Alexa 488 goat anti-mouse (Jackson ImmunoResearch) 1:700; Alexa 568 goat anti-rabbit (Molecular Probes) 1:700; and Alexa 488 rabbit anti-goat (Molecular Probes) 1:700.

Images from whole mounted preparations of the ovaries were collected using fluorescence microscopy (Leica) and confocal laser (Leica SP5). Colocalization of the proteins marked with the anti-SCYP3 and anti-nucleolin

antibodies was performed with the Leica Application Suite of image superposition and comparison software (LasX).

Meiosis progression. To study the meiotic progression in prophase I oocytes, we analyzed the different stages of the cells during Days 5, 7, and 9 of culture, in the case of *in vivo* exposure to VZN, and Days 7 and 9 in the case of *in vitro* exposure (as the *in vitro* exposure began on Day 5). The assays were carried out by counting meiotic oocytes at different stages, immunolabeled with anti-SYCP3 antibody in whole mounted preparations of cultured ovaries. An average of 368 meiotic oocytes were studied per day and exposure; a minimum of 100 follicles were analyzed under each condition.

Statistical analysis. In the cytological and morphometric assay, data was analyzed by the Kruskal–Wallis and bilinear regression, used to determine the dosage of VZN. To compare the variables among groups exposed to VZN and controls in the meiosis progression assay, the statistical analyses were carried out by one-way analysis of variance (ANOVA) with Bonferroni post hoc analysis. In the energetic metabolism analysis, one-way ANOVA test was used followed by Tukey's and Dunnett post hoc analysis. The data was processed using Seahorse Wave Desktop Software. SPSS Statistics software was used for all statistical analyses.

Received: 13 July 2020; Accepted: 12 October 2020

Published online: 22 October 2020

References

1. Van Blerkom J. Intrinsic and extrinsic patterns of molecular differentiation during Oogenesis, Embryogenesis, and Organogenesis in Mammals. In: *Cellular and Molecular Aspects of Implantation*, (ed Glasser S. R., Bullock D. W.) (Springer, Boston, MA, 1981).
2. Kurus, M., Karakaya, C., Karalok, M. H., To, G. & Johnson, J. The control of oocyte survival by intrinsic and extrinsic factors. *Adv. Exp. Med. Biol.* **761**, 7–18 (2013).
3. Gilchrist, R. B., Ritter, L. J. & Armstrong, D. T. Oocyte-somatic cell interactions during follicle development in mammals. *Anim. Reprod. Sci.* **82–83**, 431–446 (2004).
4. Bristol-Gould, S. K. *et al.* Postnatal regulation of germ cells by activin: the establishment of the initial follicle pool. *Dev. Biol.* **298**, 132–148 (2006).
5. Saitou, M. & Yamaji, M. Primordial germ cells in mice. *Cold Spring Harb. Perspect. Biol.* **4**, a008375 (2012).
6. Arora, R. *et al.* Meiotic onset is reliant on spatial distribution but independent of germ cell number in the mouse ovary. *J. Cell Sci.* **129**, 2493–2499 (2016).
7. Pepling, M. E. & Spradling, A. C. Female mouse germ cells form synchronously dividing cysts. *Development* **125**, 3323–3328 (1998).
8. Bristol-Gould, S. & Woodruff, T. K. Folliculogenesis in the domestic cat (*Felis catus*). *Theriogenology* **66**, 5–13 (2006).
9. Pepling, M. E. Follicular assembly: mechanisms of action. *Reproduction* **143**, 139–149 (2012).
10. Allard, P. & Colaiacovo, M. P. Bisphenol A impairs the double-strand break repair machinery in the germline and causes chromosome abnormalities. *Proc. Natl. Acad. Sci. USA* **107**, 20405–20410 (2010).
11. Shin, N., Cuenca, L., Karthikraj, R., Kannan, K. & Colaiacovo, M. P. Assessing effects of germline exposure to environmental toxicants by high-throughput screening in *C. elegans*. *PLoS Genet.* **15**, e1007975 (2019).
12. Susiarjo, M., Hassold, T. J., Freeman, E. & Hunt, P. A. Bisphenol A exposure in utero disrupts early oogenesis in the mouse. *PLoS Genet.* **3**, e5 (2007).
13. Hunt, P. A. *et al.* Bisphenol A alters early oogenesis and follicle formation in the fetal ovary of the rhesus monkey. *Proc. Natl. Acad. Sci. USA* **109**, 17525–17530 (2012).
14. Toppari, J. *et al.* Male reproductive health and environmental xenoestrogens. *Environ. Health Perspect.* **104**(Suppl 4), 741–803 (1996).
15. Lopez-Casas, P. P. *et al.* The effects of different endocrine disruptors defining compound-specific alterations of gene expression profiles in the developing testis. *Reprod. Toxicol.* **33**, 106–115 (2012).
16. Hunt, P. A., Sathyanarayana, S., Fowler, P. A. & Trasande, L. Female reproductive disorders, diseases, and costs of exposure to endocrine disrupting chemicals in the European Union. *J. Clin. Endocrinol. Metab.* **101**, 1562–1570 (2016).
17. Brieno-Enriquez, M. A. *et al.* Gene expression is altered after bisphenol A exposure in human fetal oocytes *in vitro*. *Mol. Hum. Reprod.* **18**, 171–183 (2012).
18. Prizant, H., Gleicher, N. & Sen, A. Androgen actions in the ovary: balance is key. *J. Endocrinol.* **222**, R141–151 (2014).
19. Walters, K. A., Allan, C. M. & Handelsman, D. J. Androgen actions and the ovary. *Biol. Reprod.* **78**, 380–389 (2008).
20. Liu, Y. *et al.* The BMP4-Smad signaling pathway regulates hyperandrogenism development in a female mouse model. *J. Biol. Chem.* **292**, 11740–11750 (2017).
21. Kelce, W. R., Monosson, E., Gamcsik, M. P., Laws, S. C. & Gray, L. E. Jr. Environmental hormone disruptors: evidence that vinclozolin developmental toxicity is mediated by antiandrogenic metabolites. *Toxicol. Appl. Pharmacol.* **126**, 276–285 (1994).
22. van Ravenzwaay, B., Kolle, S. N., Ramirez, T. & Kamp, H. G. Vinclozolin: a case study on the identification of endocrine active substances in the past and a future perspective. *Toxicol. Lett.* **223**, 271–279 (2013).
23. Brieno-Enriquez, M. A. *et al.* Exposure to endocrine disruptor induces transgenerational epigenetic deregulation of microRNAs in primordial germ cells. *PLoS ONE* **10**, e0124296 (2015).
24. Skinner, M. K. Endocrine disruptors in 2015: epigenetic transgenerational inheritance. *Nat. Rev. Endocrinol.* **12**, 68–70 (2016).
25. Buckley, J., Willingham, E., Agras, K. & Baskin, L. S. Embryonic exposure to the fungicide vinclozolin causes virilization of females and alteration of progesterone receptor expression *in vivo*: an experimental study in mice. *Environ. Health* **5**, 4 (2006).
26. Morohaku, K. *et al.* Complete *in vitro* generation of fertile oocytes from mouse primordial germ cells. *Proc. Natl. Acad. Sci. USA* **113**, 9021–9026 (2016).
27. Morohaku, K., Hirao, Y. & Obata, Y. Development of fertile mouse oocytes from mitotic germ cells *in vitro*. *Nat. Protoc.* **12**, 1817–1829 (2017).
28. Martin, J. Seeing the full picture: advances in 3D cell culture microscopy. *Biotechniques* **69**, 77–79 (2020).
29. Grive, K. J. & Freiman, R. N. The developmental origins of the mammalian ovarian reserve. *Development* **142**, 2554–2563 (2015).
30. Hirschfeld, A. N. Development of follicles in the mammalian ovary. *Int Rev. Cytol.* **124**, 43–101 (1991).
31. Medvedev, S., Pan, H. & Schultz, R. M. Absence of MSY2 in mouse oocytes perturbs oocyte growth and maturation, RNA stability, and the transcriptome. *Biol. Reprod.* **85**, 575–583 (2011).

32. Gu, W. *et al.* Mammalian male and female germ cells express a germ cell-specific Y-Box protein, MSY2. *Biol. Reprod.* **59**, 1266–1274 (1998).
33. Soyak, S. M., Amleh, A. & Dean, J. FIGalpha, a germ cell-specific transcription factor required for ovarian follicle formation. *Development* **127**, 4645–4654 (2000).
34. Wen, J. *et al.* GSK-3beta protects fetal oocytes from premature death via modulating Tap63 expression in mice. *BMC Biol.* **17**, 23 (2019).
35. Alam, M. H. & Miyano, T. Interaction between growing oocytes and granulosa cells in vitro. *Reprod. Med. Biol.* **19**, 13–23 (2020).
36. Alsheimer, M., Baier, A., Schramm, S., Schutz, W. & Benavente, R. Synaptonemal complex protein SYCP3 exists in two isoforms showing different conservation in mammalian evolution. *Cytogenet. Genome Res.* **128**, 162–168 (2010).
37. Ortega, S. *et al.* Cyclin-dependent kinase 2 is essential for meiosis but not for mitotic cell division in mice. *Nat. Genet.* **35**, 25–31 (2003).
38. Xie, H. L. *et al.* Effects of glucose metabolism during in vitro maturation on cytoplasmic maturation of mouse oocytes. *Sci. Rep.* **6**, 20764 (2016).
39. Guntur, A. R., Le, P. T., Farber, C. R. & Rosen, C. J. Bioenergetics during calvarial osteoblast differentiation reflect strain differences in bone mass. *Endocrinology* **155**, 1589–1595 (2014).
40. Qin, Y. *et al.* NOBOX homeobox mutation causes premature ovarian failure. *Am. J. Hum. Genet.* **81**, 576–581 (2007).
41. Choi, Y. & Rajkovic, A. Genetics of early mammalian folliculogenesis. *Cell. Mol. Life Sci.* **63**, 579–590 (2006).
42. San-Segundo, P. A. & Roeder, G. S. Pch2 links chromatin silencing to meiotic checkpoint control. *Cell* **97**, 313–324 (1999).
43. Visintin, R. & Amon, A. The nucleolus: the magician's hat for cell cycle tricks. *Curr. Opin. Cell Biol.* **12**, 372–377 (2000).
44. Anway, M. D., Memon, M. A., Uzumcu, M. & Skinner, M. K. Transgenerational effect of the endocrine disruptor vinclozolin on male spermatogenesis. *J. Androl.* **27**, 868–879 (2006).
45. Clement, T. M., Savenkova, M. I., Settles, M., Anway, M. D. & Skinner, M. K. Alterations in the developing testis transcriptome following embryonic vinclozolin exposure. *Reprod. Toxicol.* **30**, 353–364 (2010).
46. Nilsson, E. E., Anway, M. D., Stanfield, J. & Skinner, M. K. Transgenerational epigenetic effects of the endocrine disruptor vinclozolin on pregnancies and female adult onset disease. *Reproduction* **135**, 713–721 (2008).
47. Pesce, M., Farrace, M. G., Piacentini, M., Dolci, S. & De Felici, M. Stem cell factor and leukemia inhibitory factor promote primordial germ cell survival by suppressing programmed cell death (apoptosis). *Development* **118**, 1089–1094 (1993).
48. McClellan, K. A., Gosden, R. & Taketo, T. Continuous loss of oocytes throughout meiotic prophase in the normal mouse ovary. *Dev. Biol.* **258**, 334–348 (2003).
49. Ene, A. C., Park, S., Edelmann, W. & Taketo, T. Caspase 9 is constitutively activated in mouse oocytes and plays a key role in oocyte elimination during meiotic prophase progression. *Dev. Biol.* **377**, 213–223 (2013).
50. Rodrigues, P., Limback, D., McGinnis, L. K., Plancha, C. E. & Albertini, D. F. Multiple mechanisms of germ cell loss in the perinatal mouse ovary. *Reproduction* **137**, 709–720 (2009).
51. Shen, S., van den Brink, C. E., Kruijer, W. & van der Saag, P. T. Embryonic stem cells stably transfected with mRAR beta 2-lacZ exhibit specific expression in chimeric embryos. *Int. J. Dev. Biol.* **36**, 465–476 (1992).
52. Koubova, J. *et al.* Retinoic acid regulates sex-specific timing of meiotic initiation in mice. *Proc. Natl. Acad. Sci. USA* **103**, 2474–2479 (2006).
53. Tedesco, M., Desimio, M. G., Klinger, F. G., De Felici, M. & Farini, D. Minimal concentrations of retinoic acid induce stimulation by retinoic acid 8 and promote entry into meiosis in isolated pregonadal and gonadal mouse primordial germ cells. *Biol. Reprod.* **88**, 145 (2013).
54. Wilson, C. M. & McPhaul, M. J. A and B forms of the androgen receptor are expressed in a variety of human tissues. *Mol. Cell. Endocrinol.* **120**, 51–57 (1996).
55. Pan, B. & Li, J. The art of oocyte meiotic arrest regulation. *Reprod. Biol. Endocrinol.* **17**, 8 (2019).
56. Young, J. M. & McNeilly, A. S. Theca: the forgotten cell of the ovarian follicle. *Reproduction* **140**, 489–504 (2010).
57. Lyon, M. F., Glenister, P. H. & Lamoreux, M. L. Normal spermatozoa from androgen-resistant germ cells of chimaeric mice and the role of androgen in spermatogenesis. *Nature* **258**, 620–622 (1975).
58. Selva, D. M. *et al.* Meiotic arrest and germ cell apoptosis in androgen-binding protein transgenic mice. *Endocrinology* **141**, 1168–1177 (2000).
59. Cohen, P. E., Pollack, S. E. & Pollard, J. W. Genetic analysis of chromosome pairing, recombination, and cell cycle control during first meiotic prophase in mammals. *Endocr. Rev.* **27**, 398–426 (2006).
60. Chang, C., Lee, S. O., Wang, R. S., Yeh, S. & Chang, T. M. Androgen receptor (AR) physiological roles in male and female reproductive systems: lessons learned from AR-knockout mice lacking AR in selective cells. *Biol. Reprod.* **89**, 1–16 (2013).
61. Dumollard, R., Duchon, M. & Carroll, J. The role of mitochondrial function in the oocyte and embryo. *Curr. Top. Dev. Biol.* **77**, 21–49 (2007).
62. Prough, R. A., Clark, B. J. & Klinge, C. M. Novel mechanisms for DHEA action. *J. Mol. Endocrinol.* **56**, R139–155 (2016).
63. Klinge, C. M. Estrogenic control of mitochondrial function. *Redox Biol.* **31**, 101435 (2020).
64. Marroqui, L. *et al.* Mitochondria as target of endocrine-disrupting chemicals: implications for type 2 diabetes. *J. Endocrinol.* **239**, R27–R45 (2018).
65. Heindel, J. J. *et al.* Metabolism disrupting chemicals and metabolic disorders. *Reprod. Toxicol.* **68**, 3–33 (2017).
66. Nadal, A., Quesada, I., Tuduri, E., Nogueiras, R. & Alonso-Magdalena, P. Endocrine-disrupting chemicals and the regulation of energy balance. *Nat. Rev. Endocrinol.* **13**, 536–546 (2017).
67. Messerlian, C., Martinez, R. M., Hauser, R. & Baccarelli, A. A. “Omics” and endocrine-disrupting chemicals—new paths forward. *Nat. Rev. Endocrinol.* **13**, 740–748 (2017).
68. Buccione, R., Schroeder, A. C. & Eppig, J. J. Interactions between somatic cells and germ cells throughout mammalian oogenesis. *Biol. Reprod.* **43**, 543–547 (1990).
69. Downs, S. M., Humpherson, P. G. & Leese, H. J. Meiotic induction in cumulus cell-enclosed mouse oocytes: involvement of the pentose phosphate pathway. *Biol. Reprod.* **58**, 1084–1094 (1998).
70. Sainz de la Maza, D. *et al.* Metabolic reprogramming, autophagy, and reactive oxygen species are necessary for primordial germ cell reprogramming into pluripotency. *Oxid. Med. Cell. Longev.* **2017**, 4745252 (2017).
71. Zhao, H. *et al.* Metabolism alteration in follicular niche: the nexus among intermediary metabolism, mitochondrial function, and classic polycystic ovary syndrome. *Free Radic. Biol. Med.* **86**, 295–307 (2015).
72. Morohaku, K., Hirao, Y. & Obata, Y. Differentiation of mouse primordial germ cells into functional oocytes *in vitro*. *Ann. Biomed. Eng.* **45**, 1608–1619 (2017).
73. Sierra-Santoyo, A., Angeles-Soto, E., Lopez-Gonzalez, M. L., Harrison, R. A. & Hughes, M. F. *In vitro* metabolism of the anti-androgenic fungicide vinclozolin by rat liver microsomes. *Arch. Toxicol.* **86**, 413–421 (2012).
74. Kolle, S. N. *et al.* A testing strategy for the identification of mammalian, systemic endocrine disruptors with particular focus on steroids. *Regul. Toxicol. Pharmacol.* **63**, 259–278 (2012).
75. Environmental Protection Agency. Vinclozolin; notice of filing a pesticide petition to establish a tolerance for a certain pesticide chemical in or on food. Federal Register: 14628–14635 (2003).
76. Buckley, J., Willingham, E., Agras, K. & Baskin, L. S. Embryonic exposure to the fungicide vinclozolin causes virilization of females and alteration of progesterone receptor expression in vivo: an experimental study in mice. *Environ. Health.* **5**, 4 (2006).

77. Gray, L. E. Jr., Ostby, J., Monosson, E. & Kelce, W. R. Environmental antiandrogens: low doses of the fungicide vinclozolin alter sexual differentiation of the male rat. *Toxicol. Ind. Health* **15**, 48–64 (1999).
78. Anway, M. D., Leathers, C. & Skinner, M. K. Endocrine disruptor vinclozolin induced epigenetic transgenerational adult-onset disease. *Endocrinology* **147**, 5515–5523 (2006).
79. Guerrero-Bosagna, C. *et al.* Epigenetic transgenerational inheritance of vinclozolin induced mouse adult onset disease and associated sperm epigenome biomarkers. *Reprod. Toxicol.* **34**, 694–707 (2012).
80. Gray, L. E. Jr., Ostby, J. S. & Kelce, W. R. Developmental effects of an environmental antiandrogen: the fungicide vinclozolin alters sex differentiation of the male rat. *Toxicol. Appl. Pharmacol.* **129**, 46–52 (1994).
81. Rosen, M. P. *et al.* A quantitative assessment of follicle size on oocyte developmental competence. *Fertil. Steril.* **90**, 684–690 (2008).

Acknowledgements

We thank Agilent Technologies and Instituto de Investigaciones Clínicas, H. Clínico San Carlos for facilitating the use of the Seahorse XFp device; R. Shultz, (U. Pennsylvania) for the anti-MSY2 antibody; A. Rajkovic (U. Pittsburgh) for the NOBOX antibody; and L. Gil-Alberdi, (U. Alfonso X el Sabio) for the anti-nucleolin antibody. We acknowledge technical support from the personnel of the Animal Facility, Confocal Microscopy and Cell Culture at the Centro de Investigaciones Biológicas Margarita Salas (CSIC). We want to thank Bruce Campbell and Timothy Robinette for proofreading the manuscript.

Author contributions

S.G.-S., M.B.-E. and J. M. conceived and designed the experiments and analysis. S.G.-S., O.B. and E.R. perform the experiments and analyzed the data. S.G.-S., M.B.-E. and J. M. assessed the results and wrote the manuscript. All authors read and approved the final version of the manuscript.

Funding

This study was supported by the Agencia Estatal de Investigación; Ministerio de Ciencia, Innovación y Universidades (BFU2017-87095-R), Spain. Miguel A. Briño-Enriquez was supported by Eunice Kennedy Shriver National Institute of Child Health and Human Development (R00HD090289) and the Magee Auxiliary Research Scholar (MARS) endowment.

Competing interests

The authors declare no competing interests.

Additional information

Supplementary information is available for this paper at <https://doi.org/10.1038/s41598-020-75116-3>.

Correspondence and requests for materials should be addressed to J.d.M.

Reprints and permissions information is available at www.nature.com/reprints.

Publisher's note Springer Nature remains neutral with regard to jurisdictional claims in published maps and institutional affiliations.



Open Access This article is licensed under a Creative Commons Attribution 4.0 International License, which permits use, sharing, adaptation, distribution and reproduction in any medium or format, as long as you give appropriate credit to the original author(s) and the source, provide a link to the Creative Commons licence, and indicate if changes were made. The images or other third party material in this article are included in the article's Creative Commons licence, unless indicated otherwise in a credit line to the material. If material is not included in the article's Creative Commons licence and your intended use is not permitted by statutory regulation or exceeds the permitted use, you will need to obtain permission directly from the copyright holder. To view a copy of this licence, visit <http://creativecommons.org/licenses/by/4.0/>.

© The Author(s) 2020